Electronic Supplementary Material (ESI) for Chemical Science.

Supplementary Information for: Unexpected Inverse Correlations and Cooperativity in Ion-pair Phase Transfer

Nitesh Kumar[*,†] and Aurora E. Clark[*,†,‡]

†*Department of Chemistry, Washington State University, Pullman, Washington 99164, United States.*

‡*Pacific Northwest National Laboratory, Richland, WA*

E-mail: nitesh.kumar@wsu.edu; auclark@wsu.edu

List of Figures

List of Tables

Contents

S.1 Computational Methods

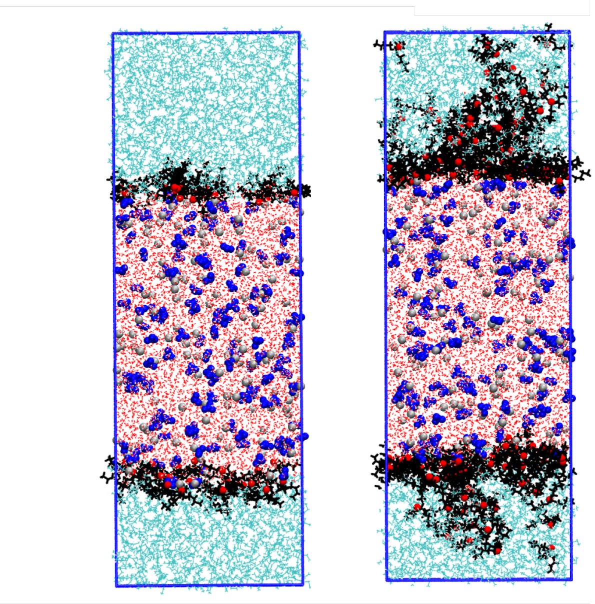

Figure S1: Schematic illustration of the electrolyte/TBP/hexane systems with 10%, 30% and 50% TBP v/v in the organic phase and 1 M $LiNO_3$ in the aqueous phase. Each system consists of two interfaces.

Table S1: The compositions of the systems simulated in this study with the equilibrated system compositions.

H_2O	n-C_6H_{14}	TBP	Li^+	$NO_3{}^-$	X × Y × Z Å^3
7055	890	48	130	130	52.9135 × 52.9135 × 157.0055
6945	890	48	260	260	52.9630 × 52.9630 × 157.1526
6754	890	48	390	390	52.8316 × 52.8316 × 156.7627
6685	890	48	520	520	53.0722 × 53.0722 × 157.4766
6555	890	48	650	650	53.0618 × 53.0618 × 157.4457
7055	692	143	130	130	52.6878 × 52.6878 × 156.3359
6945	692	143	260	260	52.8492 × 52.8492 × 156.8150
6754	692	143	390	390	52.6805 × 52.6805 × 156.3143
6685	692	143	520	520	52.8586 × 52.8586 × 156.8428
6555	692	143	650	650	52.9818 × 52.9818 × 157.2083
7055	475	238	130	130	52.3216 × 52.3216 × 155.2492
6945	475	238	260	260	52.4785 × 52.4785 × 155.7149
6754	475	238	390	390	52.3723 × 52.3723 × 156.2584
6685	475	238	520	520	52.5964 × 52.5964 × 156.0647
6555	475	238	650	650	52.7689 × 52.7689 × 156.5766

Table S2: Lennard-Jones parameters and charges for ions.

Cation	Charge(e)	ϵ (kJ/mol)	σ(nm)
Li	0.900	0.0765672	0.202590
N	0.5634	0.71128	0.315
O	-0.4878	0.882824	0.286

S.1.1 Discussion of Force Field Benchmarking

The associated radial distribution functions as a function of electrolyte concentration are presented in Figure S2 and as a cross-check to ensure that the small ECC for Li^+ and $NO_3{}^-$ will not modify the results of the current work, first principle molecular dynamics simulations were performed to calculate bulk Li^+ and $NO_3{}^-$ solvation. Initial boxes were constructed with 1 Li^+, 1 $NO_3{}^-$ and 64 H_2O molecules placed randomly in a cubic box of side length 12 Å. BOMD (Born-Oppenheimer molecular dynamics) simulations were performed in CP2K[2] at 300 K using the NPT ensemble and a 0.5 fs time-step for 500 ps. Last 400 ps was used for data analysis. The MOLOPT double and triple ζ basis sets[3,4] were used in conjugation with GTH pseudopotentials[5] using 400 Ry cutoff for plane wave basis with the revPBE-D3 set of functionals.[6,7] The H_2O coordination numbers around the central Li^+ and $NO_3{}^-$ ions were $\sim$ 4.0 (cutoff r = 3.0 Å) and $\sim$ 6.3 (cutoff r = 3.20 Å) respectively in the first solvation shell, which are in good agreement with those computed from the optimized force fields ($\sim$ 4.2 for Li^+ and 6.6 (2.2 per O_N) for $NO_3{}^-$). Further details and the comparisons of radial distribution functions and coordination numbers are illustrated in Figure S3. Several general features of the equilibrated system are also in good agreement with prior reports, which support the force field implementation. For example, in the system with 10 % TBP, the interfacial tension increases from $\sim$ 35 to 41 mN/m as $[LiNO_3]$ is increased from 1 to 5 M and there is a slight decrease in the interfacial width (Figure S4). Further, as the concentration of TBP sorbed to the instantaneous surface increases, the interfacial tension decreases concomitantly with an increase in the interfacial width. The observed $NO_3{}^-$ excess in the interfacial region is also consistent with the experiment (Figures S5 and S6).[8] Finally, there is excellent agreement with the predicted distribution coefficient for $LiNO_3$ and available experimental data (*vide infra*, Figure S7).

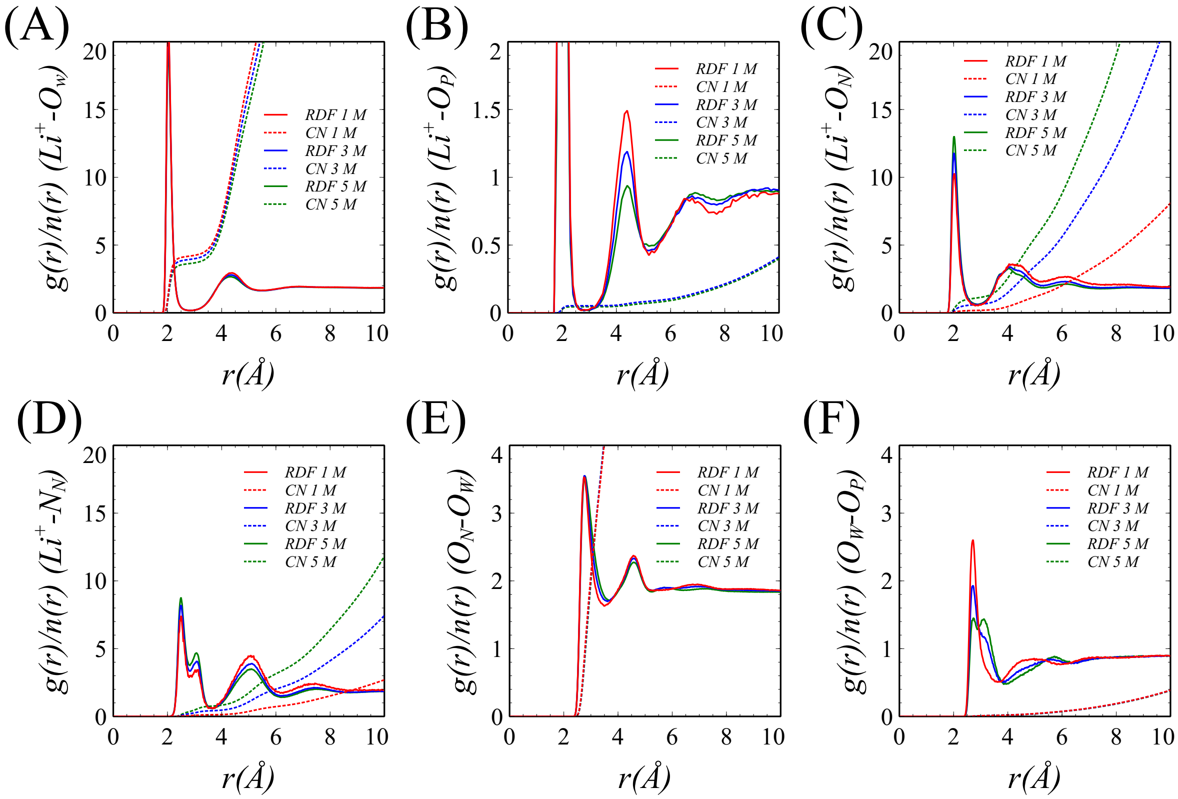

Figure S2: Classical molecular dynamics radial distribution function g(r) and coordination number n(r) variations for different atom pairs interactions at 1,3 and 5 M [$LiNO_3$] in system with 10% TBP.

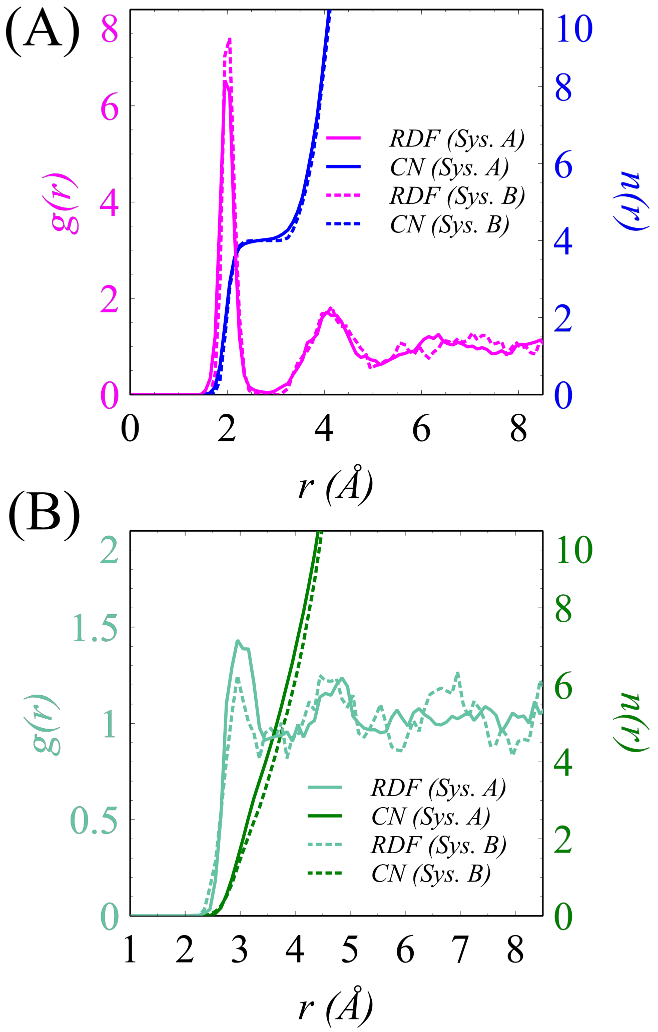

Figure S3: Pair correlation function g(r) and coordination number n(r) plots for (A) Li^+-O_W (B) O_N-O_W calculated using two AIMD systems with different basis sets and functionals. System A and B represents double (DZVP-MOLOPT-SR-GTH) and triple zeta (TZVP-MOLOPT-GTH) basis sets respectively with GTH-revPBE functionals.

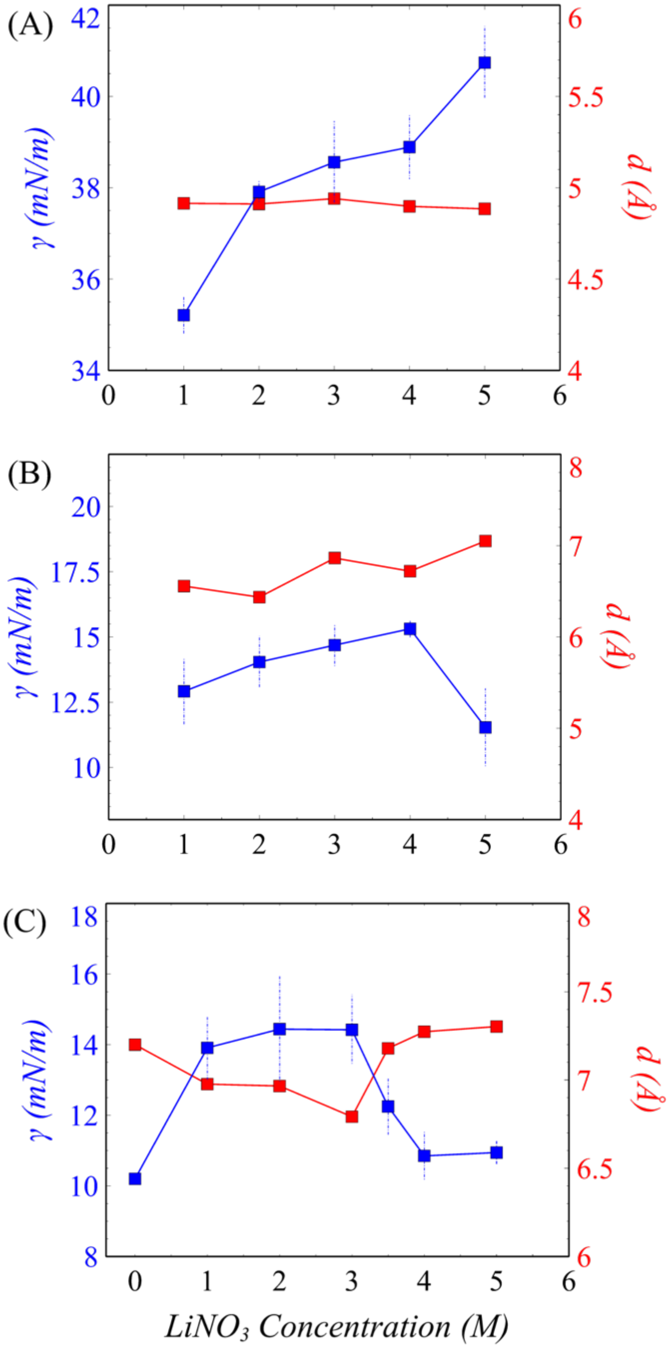

Figure S4: The electrolyte concentration ($LiNO_3$) is plotted against interfacial tension (left axis), and the fitted width of the interfacial water molecules (right axis) in the systems with (A) 10% TBP v/v in the organic phase, (B) 30% TBP v/v in the organic phase, (C) 50% TBP v/v in the organic phase. Interfacial width d was calculated from the density distribution of H_2O molecules present in the instantaneous surface, fitted to a normal distribution function with d the full width at half maximum.

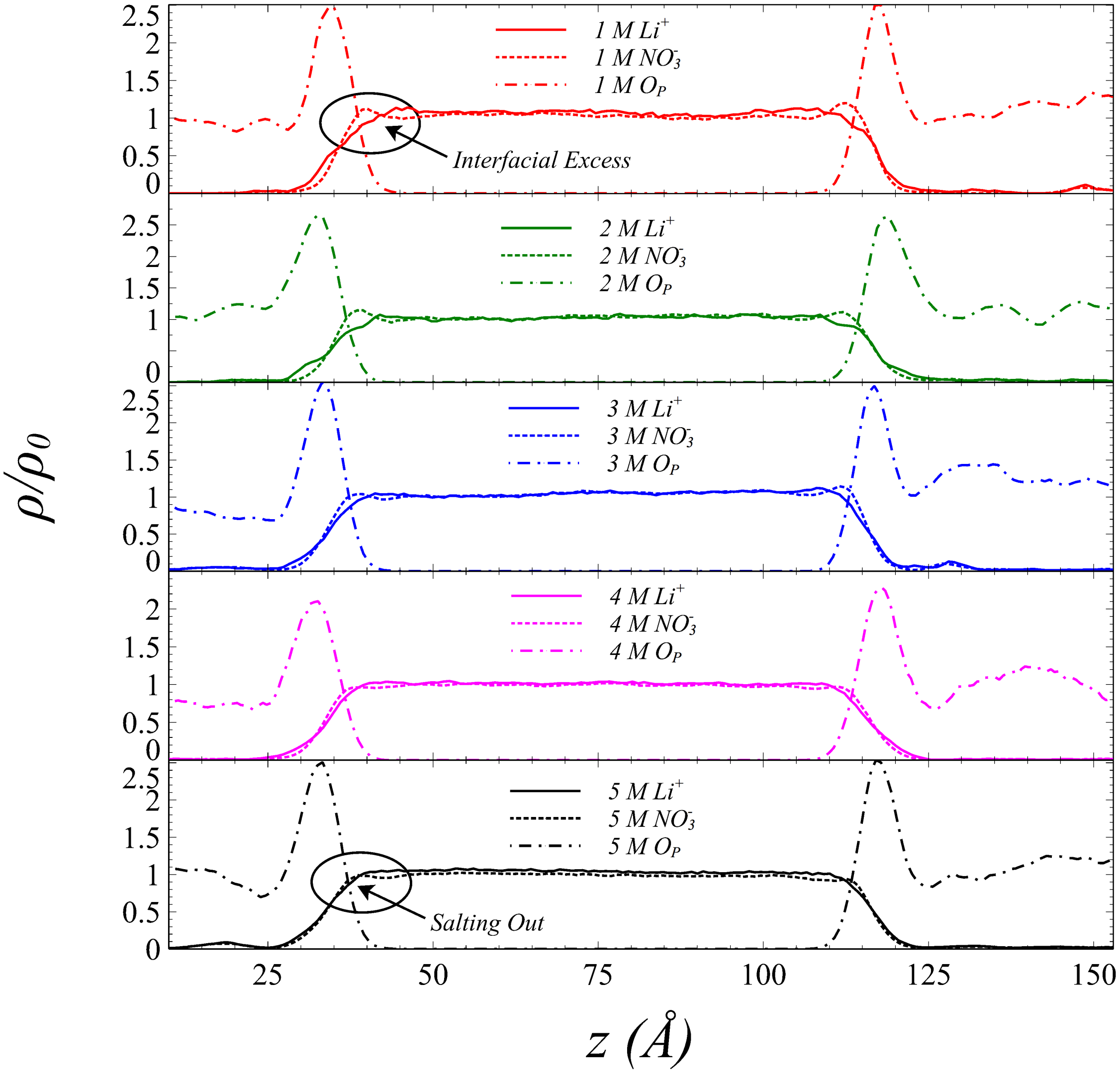

Figure S5: Normalized density profiles of Li^+, $\mathrm{NO_3}^-$ and O(TBP) in the systems with 50 % TBP in organic phase and at 1-5 M [$\mathrm{LiNO_3}$]. The densities were divided by the respective bulk densities ρ_0 for normalization.

Table S3: Distance cutoffs used for generating inter- and intra-atomic interactions in the simulated systems.

Atom 1	Atom 2	r_{12}(Å)
Li^+	O_{Water}	3.00
Li^+	$O_{Nitrate}$	2.86
Li^+	$N_{Nitrate}$	3.50
Li^+	O_{TBP}	3.00
O_{Water}	H_{Water}	2.50
O_{TBP}	H_{Water}	2.50

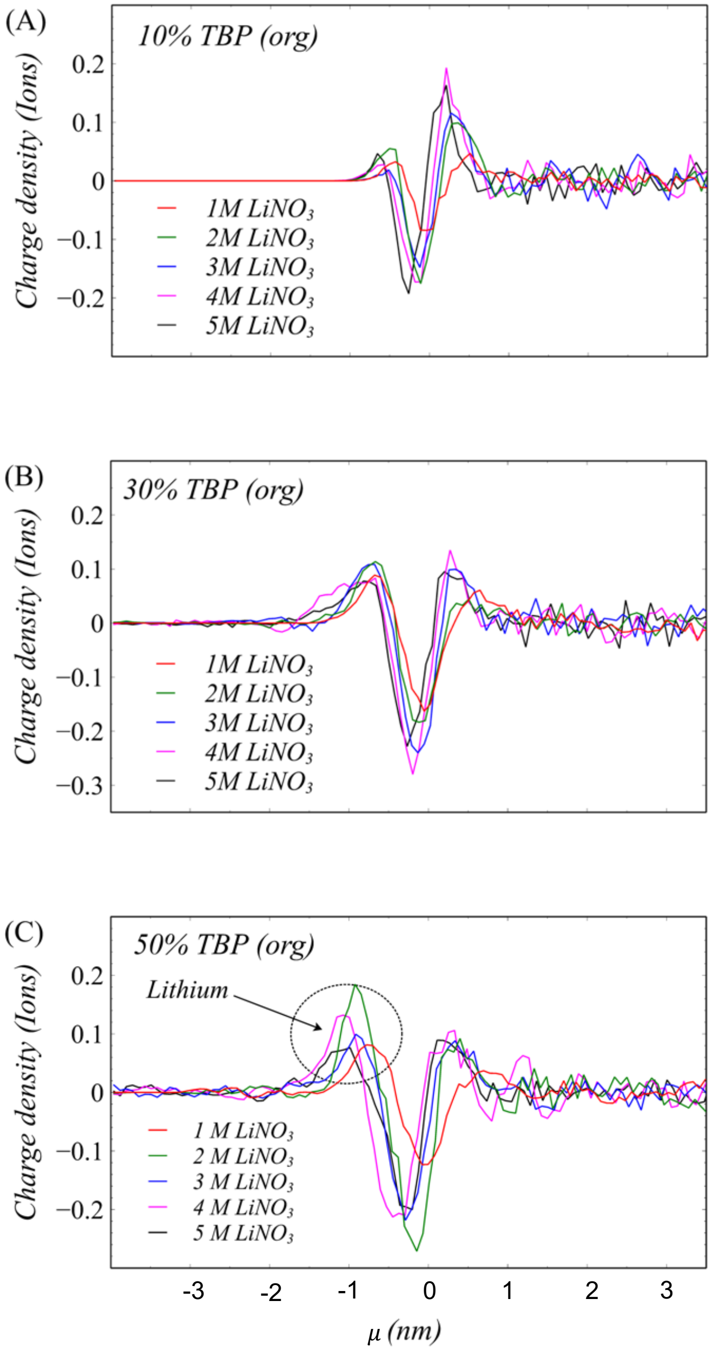

Figure S6: Electrolyte charge density distributions plotted at 1-5 M LiNO$_3$ with (A) 10 % (B) 30 % (c) 50 % v/v TBP in organic phase.

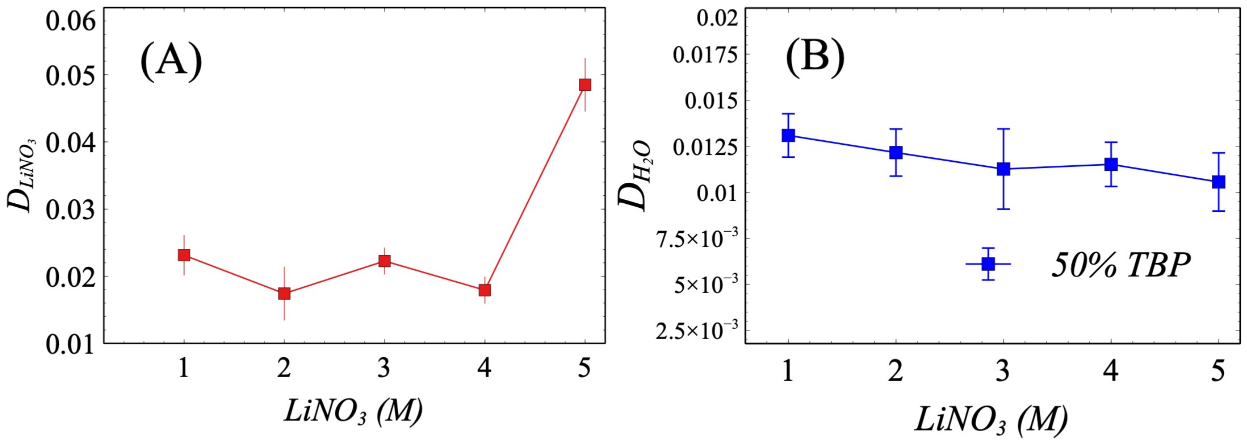

Figure S7: (A) Variations in the distribution ratio of $\mathrm{LiNO_3}$, $D_{\mathrm{LiNO_3}}$ as a function of $[\mathrm{LiNO_3}]$ in the system with 50 % TBP. (B) Variations in the distribution ratio of water $D_{\mathrm{H_2O}}$ as a function of $[\mathrm{LiNO_3}]$ in systems with 30% and 50% TBP in the organic phase.

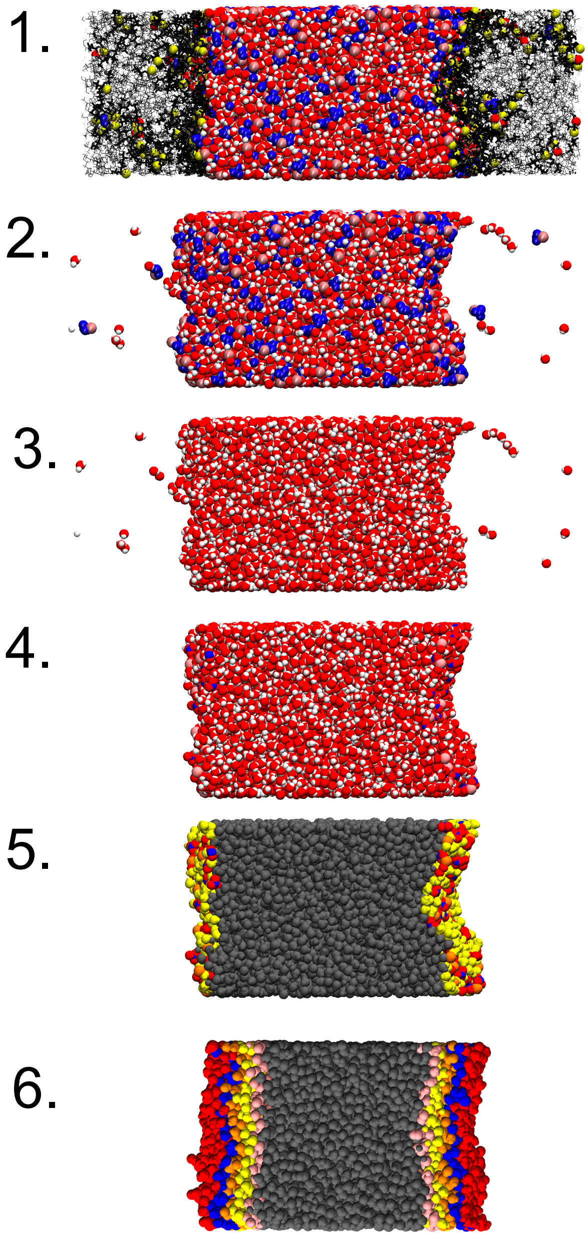

Figure S8: An illustration of the steps involved in the identification of truly interfacial molecules in the heterogeneous system with water and ion-pairs extracted into the organic phase. The steps are (1.) Separate individual snapshots from a molecular dynamics trajectory. (2.) Extract H_2O and $LiNO_3$ from the coordinate file. (3.) Apply graph theory based cluster analysis on H_2O H-bonding network to separate bulk and extracted water. (4.) Include $LiNO_3$ based on the largest H_2O cluster. (5.) Apply ITIM analysis on the electrolyte system to identify the interfacial ions and water.[1] (6.) An illustration of the instantaneous layers (L1-L5) identified using ITIM algorithm.

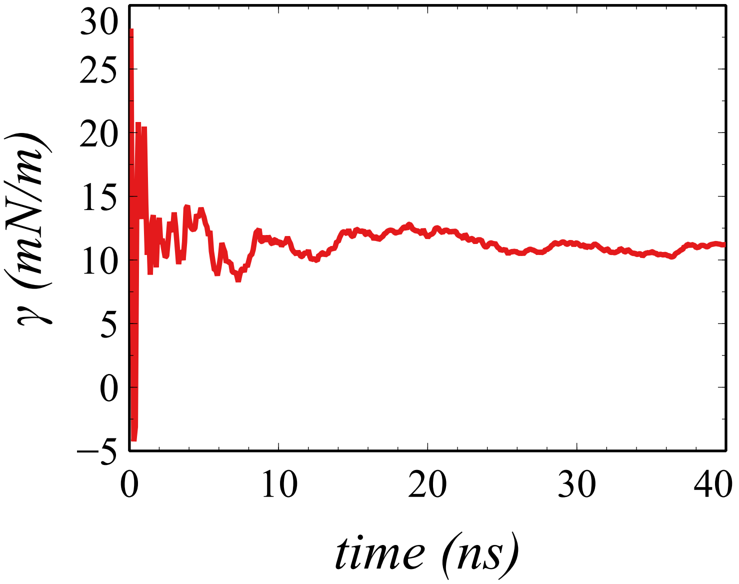

Figure S9: The time evolution of the interfacial tension in systems with 5 M $LiNO_3$ and 50% TBP.

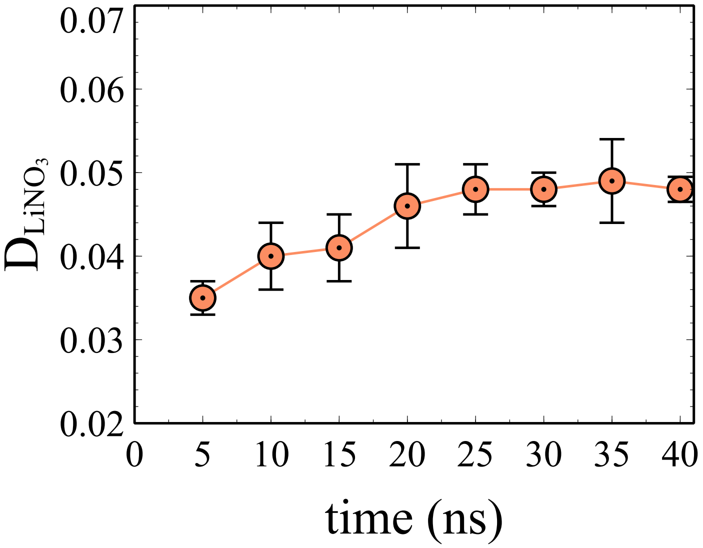

Figure S10: The variations in the distribution ratio (D) with time in systems with 5 M $LiNO_3$ and 50% TBP.

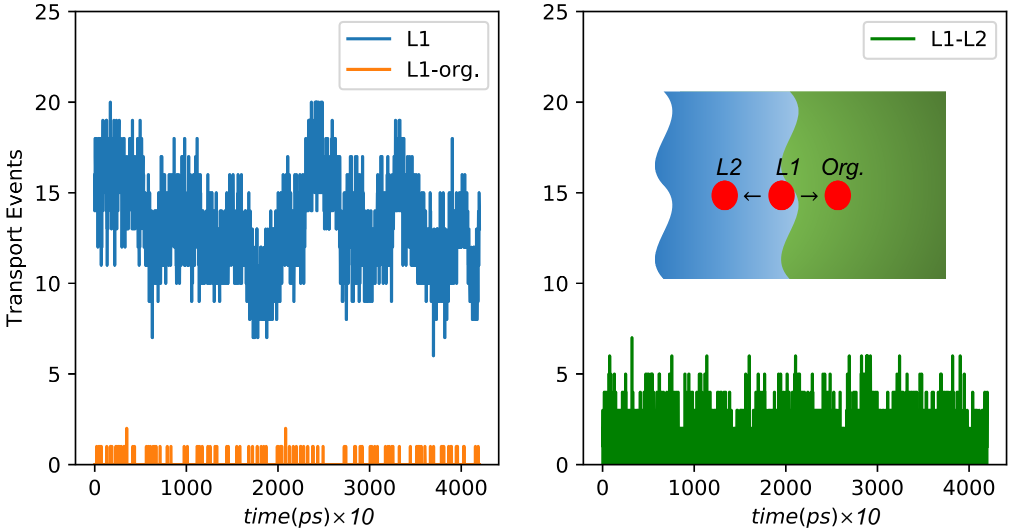

Figure S11: The time evolution of the average number of lithium transport events from the truly interfacial layer L1 to the aqueous phase layer L2 (L1 $\longrightarrow$ L2) and from L1 to the organic phase (L1 $\longrightarrow$ org) with time in the system with 1 M [$LINO_3$] and 50 % TBP in the organic phase. A schematic illustration of the equilibrium transport process is shown in the inset (right panel).

S.2 Results and Discussion

Table S4: Surface coverage of TBP per interface (TBP/Å^2) at different [LiNO$_3$]. The values are reported as $x \times 10^{-3}$ TBP/Å^2.

$LiNO_3$	10 % TBP	30 % TBP	50 % TBP
1 M	3.75 ± 0.05	15.40 ± 0.15	28.95 ± 0.34
2 M	3.13 ± 0.01	11.92 ± 0.35	21.17 ± 0.69
3 M	2.51 ± 0.06	09.79 ± 0.05	18.13 ± 0.08
4 M	2.14 ± 0.02	07.57 ± 0.06	11.52 ± 0.34
5 M	1.72 ± 0.01	06.41 ± 0.15	10.85 ± 0.42

Table S5: Ensemble average number of LiNO$_3$ and H$_2$O extracted in the organic phase in the system with 50 % TBP.

[$LiNO_3$] M	$LiNO_3$	H_2O
1	3.1	91.2
2	4.5	84.4
3	8.6	76.1
4	9.3	77.2
5	31.5	69.2

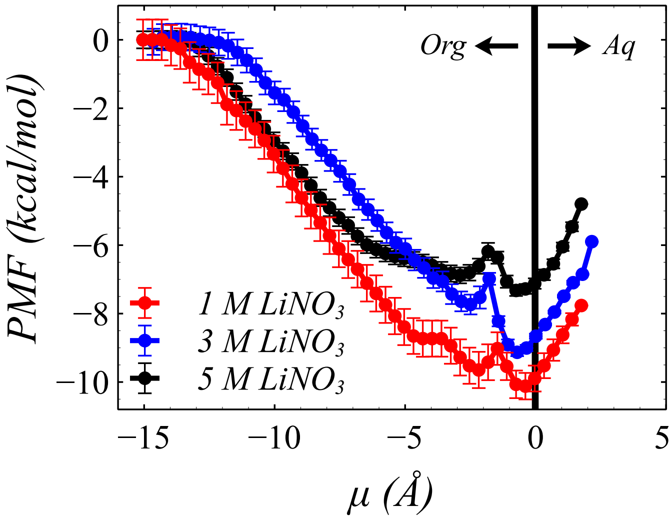

Figure S12: Free energy profiles of a single TBP adsorption (no other TBP present in the system) at the liquid/liquid surfaces with 1, 3, and 5 M [LiNO$_3$] in the aqueous phase. Negative values on the μ axis represent the organic phase. The transition state in the region μ = -1 to -2 Å shows the breakage of the water protrusion. The region μ < -5 Å represents the immediate organic phase and the region μ < -15 Å represents the bulk organic phase.

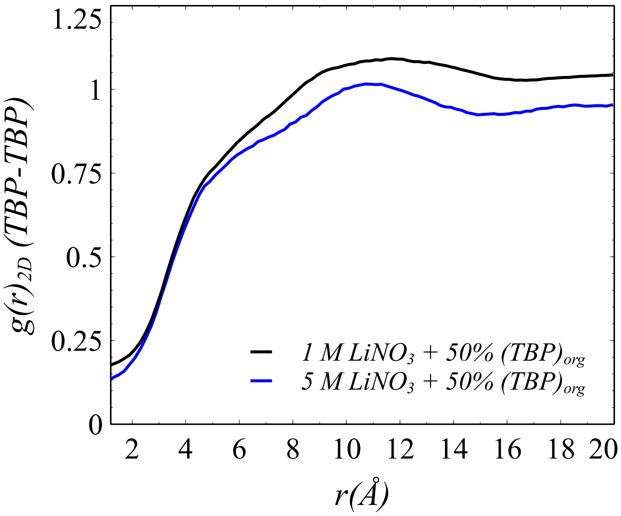

Figure S13: Comparison of the two dimensional pair correlations $g_{2D}(r)$ of the adsorbed TBP molecules plotted at various [$LiNO_3$] in the system with 50 % TBP in the organic phase.

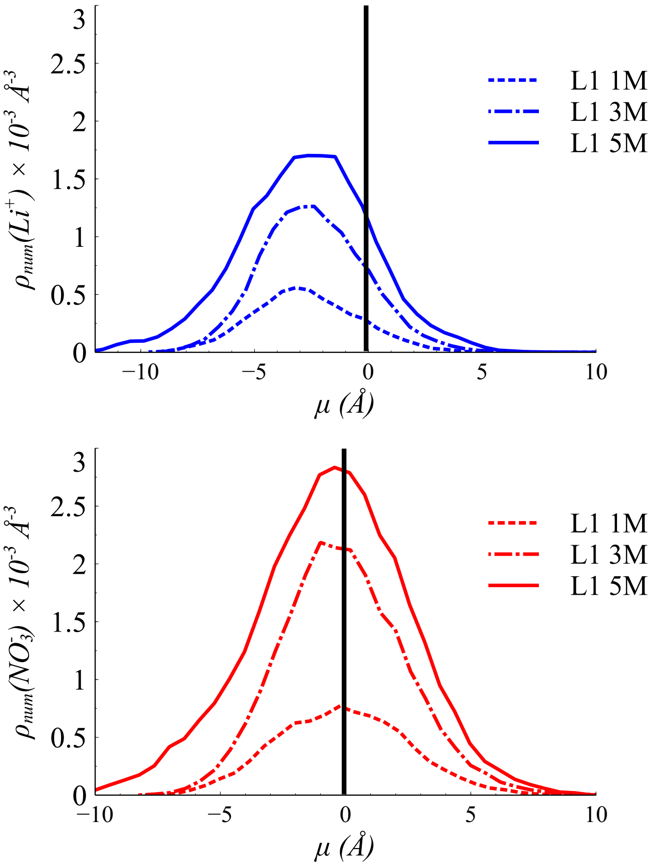

Figure S14: Distributions of (A) Li^+ and (B) NO_3^- in instantaneous surface at various [$LiNO_3$] (1, 3 and 5 M) in the systems with 50% v/v TBP in the organic phase.

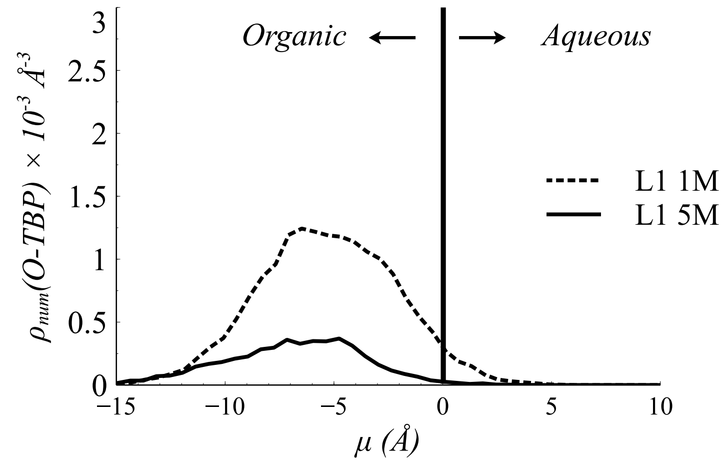

Figure S15: Distribution of TBP within the instantaneous surface at 1 and 5 M $LiNO_3$ in the systems with 50% v/v TBP in the organic phase.

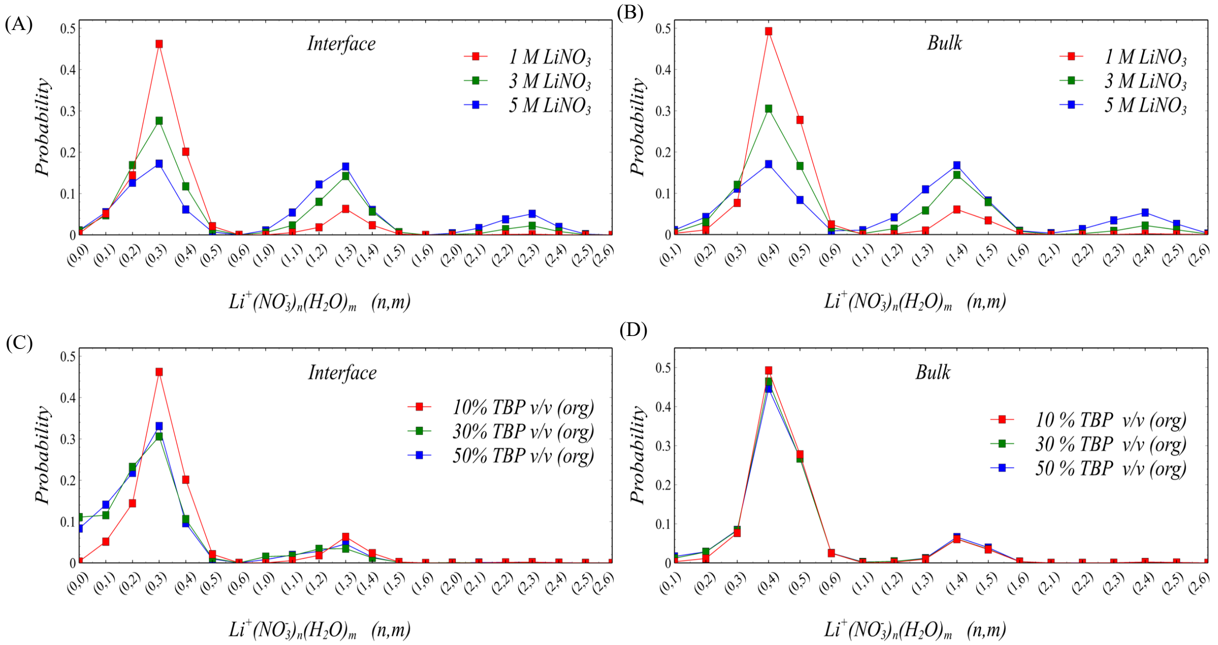

Figure S16: Total Solvation distribution of the interfacial lithium ions ($Li^+ \cdots NO_3^- \cdots H_2O$) with change in [$LiNO_3$] (A) at interface (B) in bulk in the systems with 10% TBP (C) Total solvation distribution of interfacial lithium ions (C) at interface and (D) in bulk aqueous phase with change in TBP concentration concentrations.

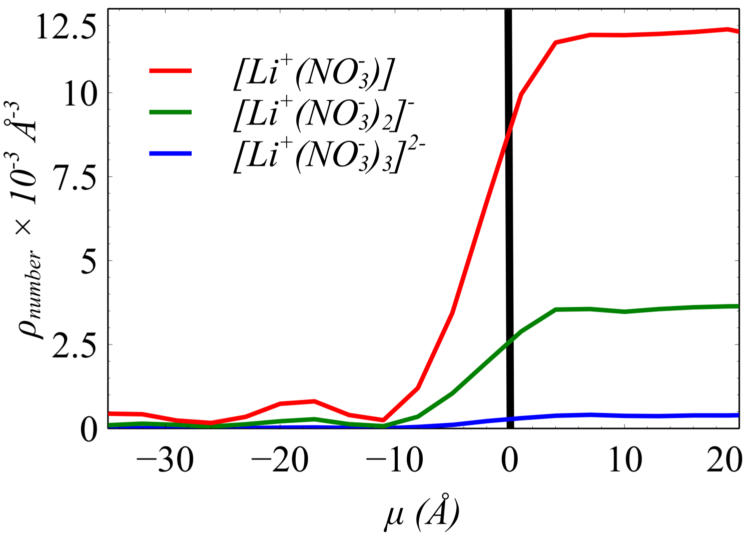

Figure S17: (A) Distribution of $Li^{+}(NO_3{}^{-})_n$ complexes along μ axis in system with 5 M $LiNO_3$ in aqueous phase and 50 % TBP in organic phase. Note that water mean density distribution is shown by black solid line.

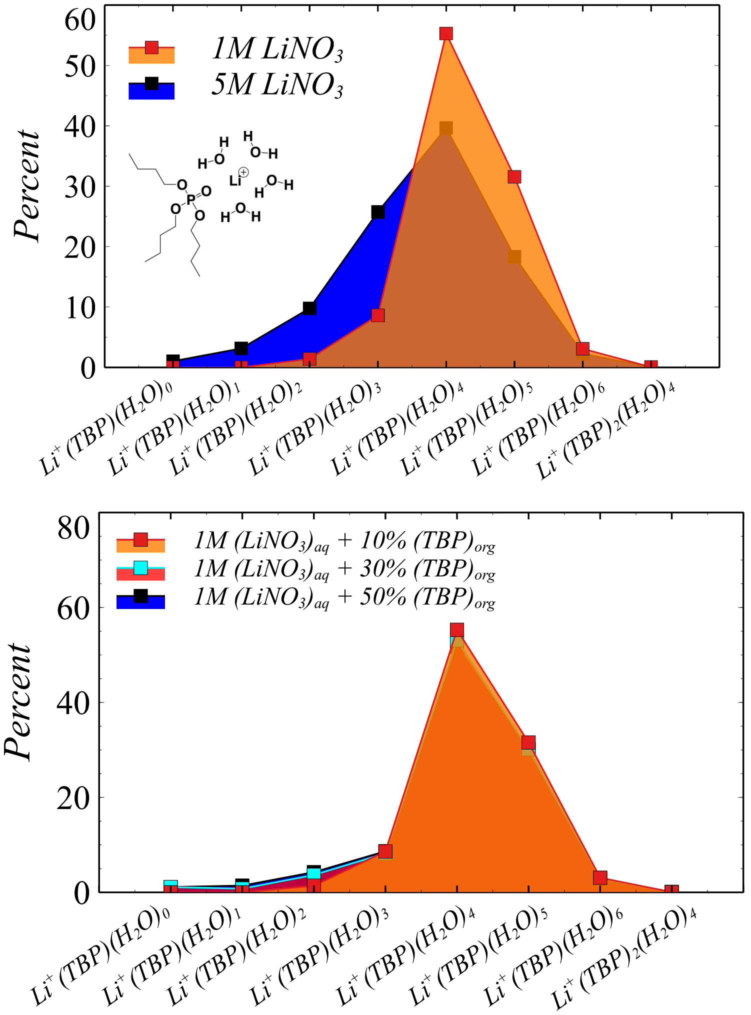

Figure S18: Upper panel: Total $Li^+(TBP)_n(H_2O)_m$ coordination number distributions of interfacial Li^+ ions with change in $LiNO_3$ concentrations in 10% TBP system. The most probable $Li^+\cdots H_2O\cdots TBP$ complex is shown in the inset. Note that the interfacial Li^+ ions were identified using ITIM algorithm. Lower panel: Total $Li^+(TBP)_n(H_2O)_m$ coordination number distributions of interfacial Li^+ ions with change in TBP concentrations.

References

(1) Kumar, N.; Servis, M. J.; Liu, Z.; Clark, A. E. Competitive Interactions at Electrolyte/Octanol Interfaces: A Molecular Perspective. *The Journal of Physical Chemistry C* **2020**, *124*, 10924–10934.

(2) Hutter, J.; Iannuzzi, M.; Schiffmann, F.; Vande Vondele, J. cp2k: atomistic simulations of condensed matter systems. *Wiley Interdisciplinary Reviews: Computational Molecular Science* **2014**, *4*, 15–25.

(3) VandeVondele, J.; Hutter, J. Gaussian basis sets for accurate calculations on molecular systems in gas and condensed phases. *The Journal of Chemical Physics* **2007**, *127*, 114105.

(4) Elstner, M.; Porezag, D.; Jungnickel, G.; Elsner, J.; Haugk, M.; Frauenheim, T.; Suhai, S.; Seifert, G. Self-consistent-charge density-functional tight-binding method for simulations of complex materials properties. *Physical Review B* **1998**, *58*, 7260.

(5) Krack, M. Pseudopotentials for H to Kr optimized for gradient-corrected exchange-correlation functionals. *Theoretical Chemistry Accounts* **2005**, *114*, 145–152.

(6) Hammer, B.; Hansen, L. B.; Nørskov, J. K. Improved adsorption energetics within density-functional theory using revised Perdew-Burke-Ernzerhof functionals. *Physical Review B* **1999**, *59*, 7413.

(7) Gerald Lippert, J. H.; Parrinello, M. A hybrid Gaussian and plane wave density functional scheme. *Molecular Physics* **1997**, *92*, 477–488.

(8) Hong, A. C.; Wren, S. N.; Donaldson, D. Enhanced surface partitioning of nitrate anion in aqueous bromide solutions. *The Journal of Physical Chemistry Letters* **2013**, *4*, 2994–2998.